



EFFECT OF INFILL STYLE AND DENSITY ON SELECTED MECHANICAL PROPERTIES OF THE CARBON FIBRE REINFORCED ABS MFD FILAMENT

M. Mucha¹, D. Sikorski², R. Szczepaniak¹, R. Bąbel¹, A. Krzyżak¹ & T. Zahorski¹

¹Faculty of Aviation, Polish Air Force University, Dywizjonu 303 Street No. 35, 08-521 Dęblin, POLAND

²41st Training Air Base, Brygady Pościgowej Street No. 5, 08-521 Dęblin, POLAND

Abstract

Carbon fiber reinforced 3D printer filaments are currently gaining popularity due to their ability to combine the exceptional ease of use typical for FDM (Fused Deposition Modeling) with the outstanding mechanical properties of CFRP (Carbon Fiber Reinforced Polymers). In this research, ABS-CF10 carbon-reinforced ABS, which is the latest product in the Stratasys company commercial offer, was investigated. The reference material was ABS-M30, which is a versatile and well-known FDM thermoplastic with a wide range of applications. The Stratasys F170 3D printer was used to produce the samples. Two different infill styles with two different infill densities were used: Sparse (35%, 80%) and Sparse Double Dense (35%, 80%). Tensile (ISO-527) and flexural (ISO-178) properties were determined using the ZwickRoell Z5.0 universal testing machine. The results indicate that both ABS and ABS-CF exhibit increased strength and stiffness with higher infill density. Carbon fiber reinforcement significantly enhances the strength and modulus of elasticity compared to neat ABS. Differences were observed between Sparse and Sparse Double Dense infill styles at the same infill densities, depending on whether ABS or ABS-CF was tested. The study highlights that CF10 Sparse 35% demonstrates superior strength and modulus of elasticity relative to the mass of the final product.

Keywords: fused deposition modeling (FDM); acrylonitrile butadiene styrene (ABS); Carbon Fiber Reinforced Polymers (CFRP); mechanical properties; 3D printing parameters

1. Introduction

Additive manufacturing (AM) represents a significant advancement in contemporary materials science. One of the most commonly used 3D printing methods is Fused Deposition Modeling (FDM), which allows for the production of items from various materials. Additionally, 3D printing plays a social role by providing access to affordable technology for those with basic technical knowledge [1]. It plays an important role in various fields, such as archaeology, by enabling the creation of colorful replicas of ancient artifacts, thereby promoting knowledge among the public while preserving invaluable relics [2].

The impact of infill patterns on the mechanical properties of 3D printing has been intensively studied [3]. Comparisons are made between different infill styles, such as rectangular and hexagonal infills [4], and various styles including Cartesian, Rhomboid, Octagonal, and Starlit structures are being investigated [5]. When there is considerable freedom in designing infill styles, optimization may require a hybrid statistical approach based on artificial intelligence [6].

ABS is renowned for its excellent resistance to environmental conditions compared to ASA, HIPS, and PLA [7]. The study of ABS prints has been the subject of numerous research efforts. Mechanical properties are often determined using three-point bending tests [8] with evaluations of failure modes [9]. Additionally, static tensile tests are conducted to assess mechanical properties, with a particular focus on evaluating printing parameters [10].

EFFECT OF INFILL STYLE AND DENSITY ON MECHANICAL PROPERTIES OF THE CFR ABS MFD FILAMENT

FRP composites are utilized in diverse applications, such as military vehicles, shelters, safety equipment during warfare, fighter jets, warships, and submarine structures [11]. The use of 3D printing with carbon fiber-reinforced filament is becoming increasingly common [12]. The significant potential of this technology is further evidenced by the ability to obtain recycled carbon fibers, which could be a game-changer in addressing the recycling issues of CFRP [13]. However, passing carbon fibers through the extruder can weaken their strength [14].

In the context of 3D printing, carbon fiber reinforcement can be used not only in ABS but also in other polymers, such as nylon [15]. Other materials used in 3D printing, such as polyamide, are also being studied for the impact of carbon fiber additives on their properties [16]. Additionally, other reinforcing fibers, such as polypropylene (PP) [17] and glass fibers [18], are also used in 3D printing.

It is essential to study materials printed using the FDM method and reinforced with carbon fiber, including conducting typical tests for plastics such as Dynamic Mechanical Analysis (DMA). DMA is a modern research tool that allows for precise measurement of viscoelastic properties or other mechanical properties of a material as a function of temperature by applying an oscillatory force to the sample [19].

2. Materials and Methods

2.1 Materials and Printing Procedures

This study employed two materials: ABS and carbon fiber-modified ABS. ABS-M30, a thermoplastic from Stratasys, was chosen for the ABS samples due to its suitability for initial prototyping and various applications in 3D printing. ABS-CF10 filament was used for samples containing carbon fibers. Depending on specific requirements, carbon fiber-reinforced ABS can replace certain metal components, enabling the creation of complex geometries that are impractical with traditional machining methods. ABS-M30 has a density of approximately 1.01 g/cm^3 , whereas CF10 has a higher density of around 1.10 g/cm^3 .

The samples were printed using a Stratasys F170 3D printer, which operates with GrabCAD Print software. Two different infill styles were utilized: Sparse and Sparse Double Dense. Additionally, two different infill densities were employed: 35% and 80%. Figure 1 illustrates the arrangement of a series of samples for static tensile testing and samples for three-point bending on the tray.

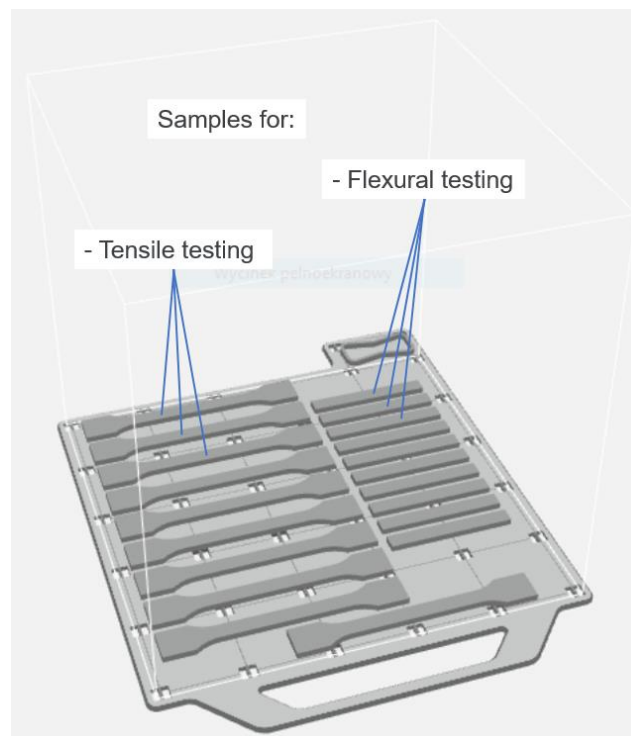


Figure 1 – Sample distribution on the tray.

2.2 Tensile and flexural testing

Determination of tensile properties was conducted according to ISO-527 standard. The samples were shaped as typical dog-bones with a cross-sectional area of 4 mm x 10 mm. Determination of flexural properties was carried out in accordance with ISO-178 standard. Rectangular samples measuring 4 mm x 10 mm x 80 mm were tested. Both tests were performed using a ZwickRoell Z5.0 universal testing machine. For the static tensile test, pneumatic grips and a ClipOn extensometer were used. During the three-point bending test, the span between specimen supports was 64 mm and the test speed was 2 mm/min. Each series consisted of 10 samples.

For each sample series, the relative mass was determined, which was estimated by the 3D printer software as the mass of the flexural testing sample divided by the mass of a sample made of pure ABS with Solid infill style, i.e., 100% infill density.

2.3 Optical microscopy

The optical microscopy examination was conducted using an Olympus BX53M device. The dark field technique was employed with an exposure time of 60 ms and a magnification of 5x.

2.4 DMA

For this study, a Netzsch 242 E Artemis device was used to conduct a three-point bending test, which is one of the most commonly performed tests in DMA. This test involves placing the sample on two supporting edges and applying a dynamic force to it. After initially analyzing the material's elastic properties, a three-point bending fixture designed for soft materials was employed. Subsequently, the sample was heated and cooled according to a preset temperature program. For this study, only the results obtained during heating the material from -70 °C to +120 °C at a heating rate of 3 K/min are presented. The force oscillated at a frequency of 1.0 Hz.

3. Results

3.1 Tensile testing

The measured values of the Young's modulus in relation to relative mass are presented in Fig. 2. Samples made of ABS-CF10 exhibit significantly greater tensile stiffness than those made of pure ABS. Additionally, the density difference between the two filaments causes the CF10 samples to be shifted to the right on the graph compared to ABS. An infill density of 80% slightly improves stiffness compared to 35%, but it also evidently increases the relative mass. Infill style does not have a significant impact on the stiffness modulus, although the application of Sparse Double Dense results in a slightly higher relative mass compared to Sparse.

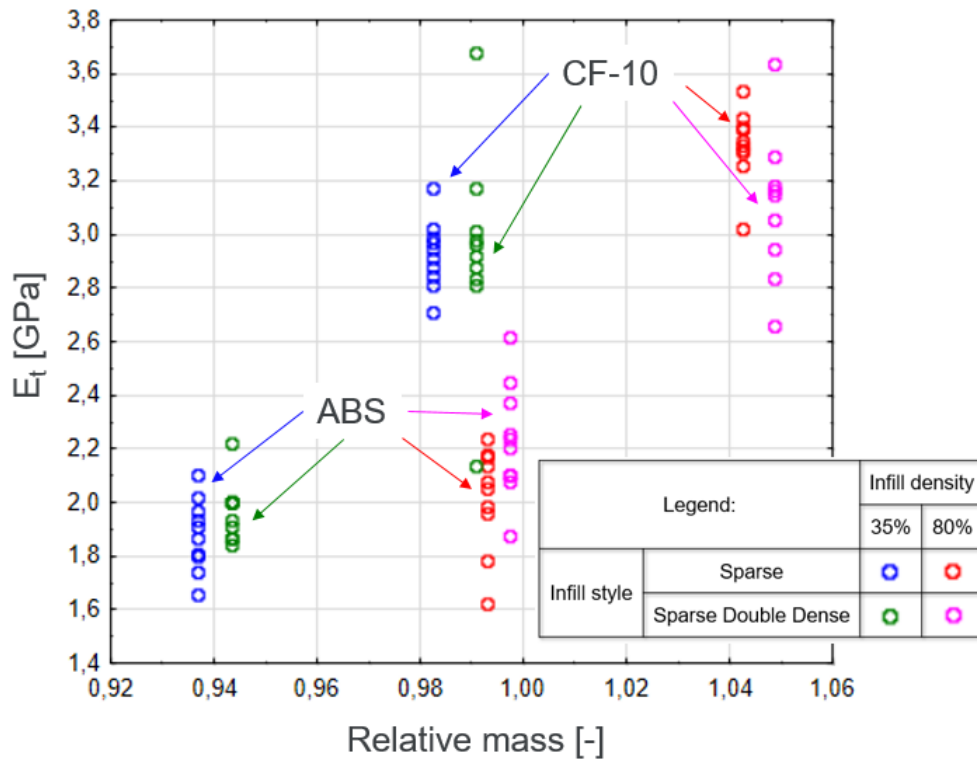


Figure 2 – Young's modulus in relation to relative mass.

The obtained tensile strength values in relation to relative mass are presented in Fig. 3. When tensile strength is considered a priority, the best properties are achieved with CF10 material using a Sparse infill style and 80% infill density. When minimizing the density of the structural material becomes increasingly important, CF10 Sparse 35% shows an advantage over CF10 Sparse Double Dense 35%, ABS Sparse 80%, and ABS Sparse Double Dense 80%.

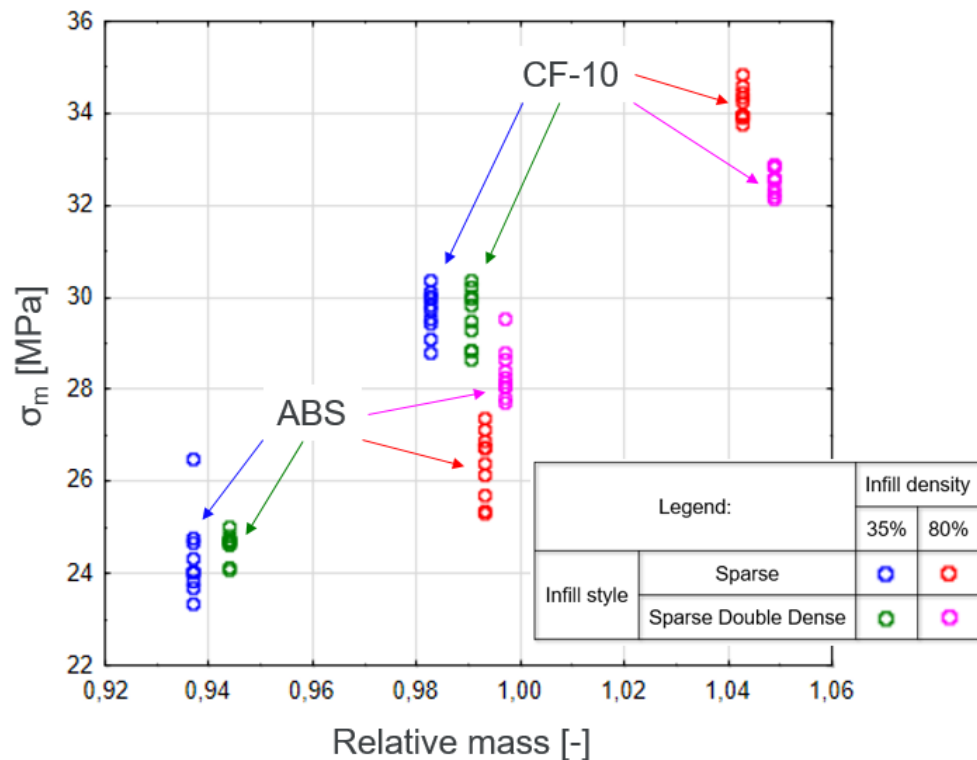


Figure 3 – Tensile strength in relation to relative mass.

3.2 Flexural testing

The obtained values of the modulus of elasticity in flexure are presented in relation to relative mass in Fig. 4. Nominally, the highest flexural modulus values—an average of 2.72 GPa with a sample mass estimated by the software to be 4.39 g—were achieved with CF10 material, using Sparse infill style and 80% infill density. CF10 Sparse 35% exhibits slightly lower flexural modulus—an average of 2.61 GPa—and a lower sample mass of 4.14 g. This represents a 5.7% decrease in mass with a 3.9% decrease in stiffness. Additionally, the graph shows less variation in the results compared to tensile stiffness.

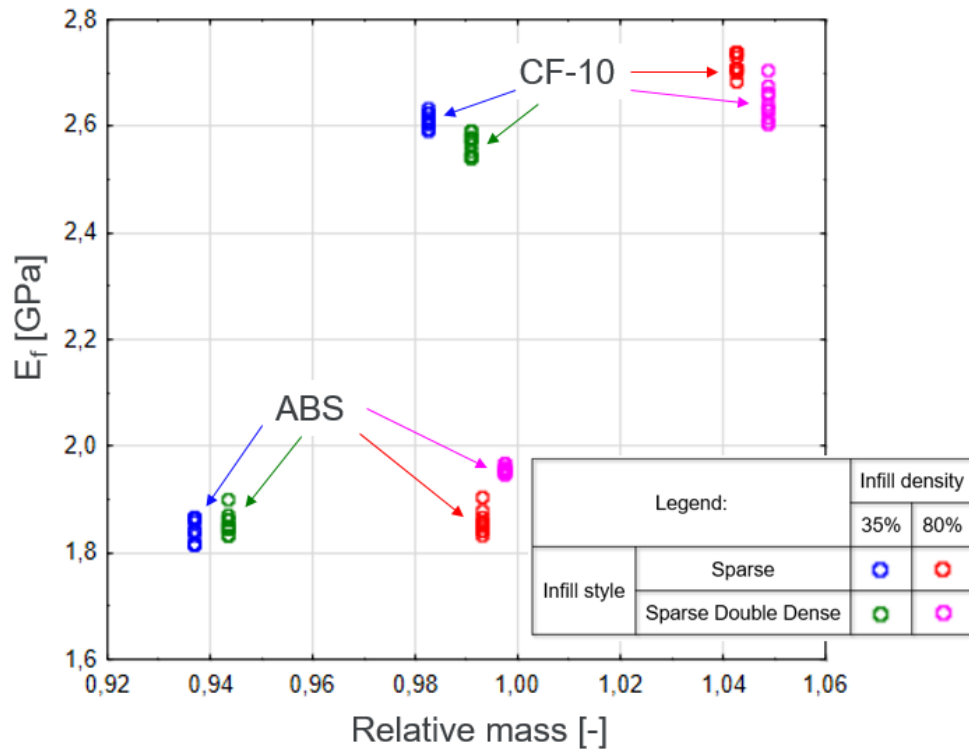


Figure 4 – Flexural modulus in relation to relative mass.

The obtained flexural strength values in relation to relative mass are presented in Fig. 5. As in previous observations, the best results were achieved with CF10 material using Sparse infill style and 80% infill density, but CF10 Sparse 35% achieved slightly lower results with a significantly lower sample mass. For both flexural modulus and flexural strength, it is more evident than in the case of tensile testing that for pure ABS, the Double Sparse infill style is more advantageous, while for ABS-CF10, the Sparse infill style yields better results.

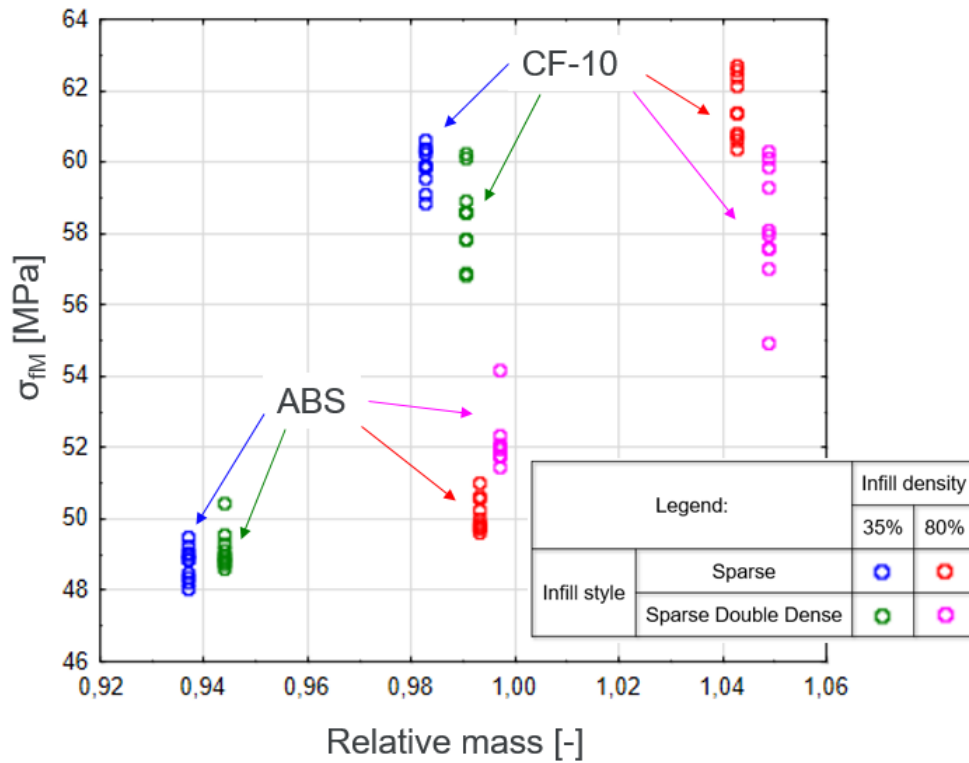


Figure 5 – Flexural strength in relation to relative mass.

3.3 Optical microscopy inspection

Optical microscopy allowed for the observation of the material's failure modes. The analyzed sample was made of ABS-CF10 with a Sparse Double Dense infill style and 80% infill density. The sample was broken during bending. Both the compressed area and the tensioned area were observed. The compressed area, compared to the tensioned area, had a less developed surface. This made it easier to focus on the area over a larger fracture surface (Fig. 6). In the image, carbon fibers are indicated by the red arrows. It is also evident that there are few voids between the filament paths (white arrows). The dominant type of failure mode is intra-layer/trans-raster failure.

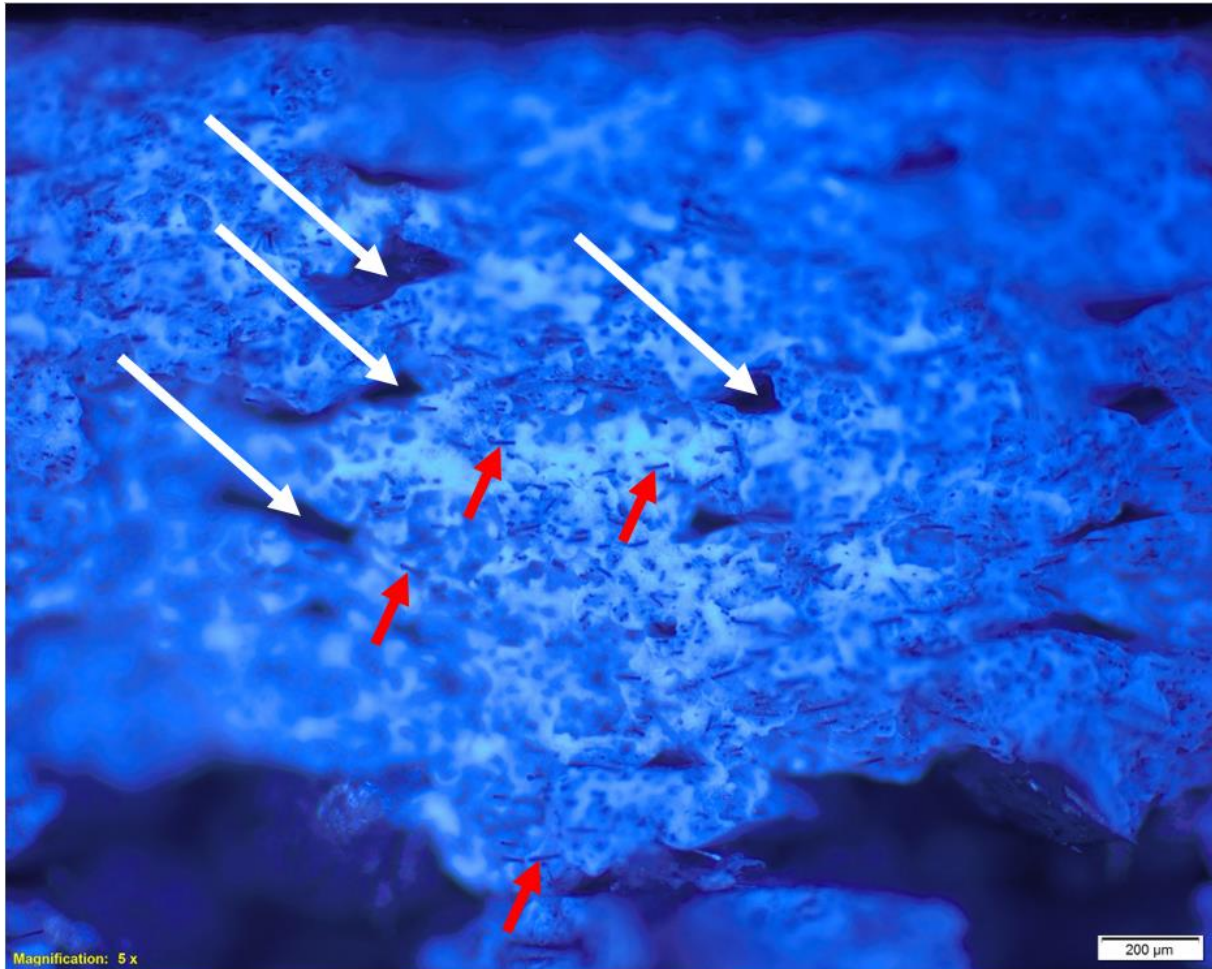


Figure 6 – Fracture of the CF10 sample damaged under compression.

In Fig. 7, the area damaged under tension is presented. Due to the developed surface, it is difficult to focus on the details. Significant voids causing the separation of individual filament paths are visible (gray arrows). It can be concluded that in addition to trans-raster failure, there is also inter-raster bond failure. Fibers that have been pulled out are indicated with gold arrows.

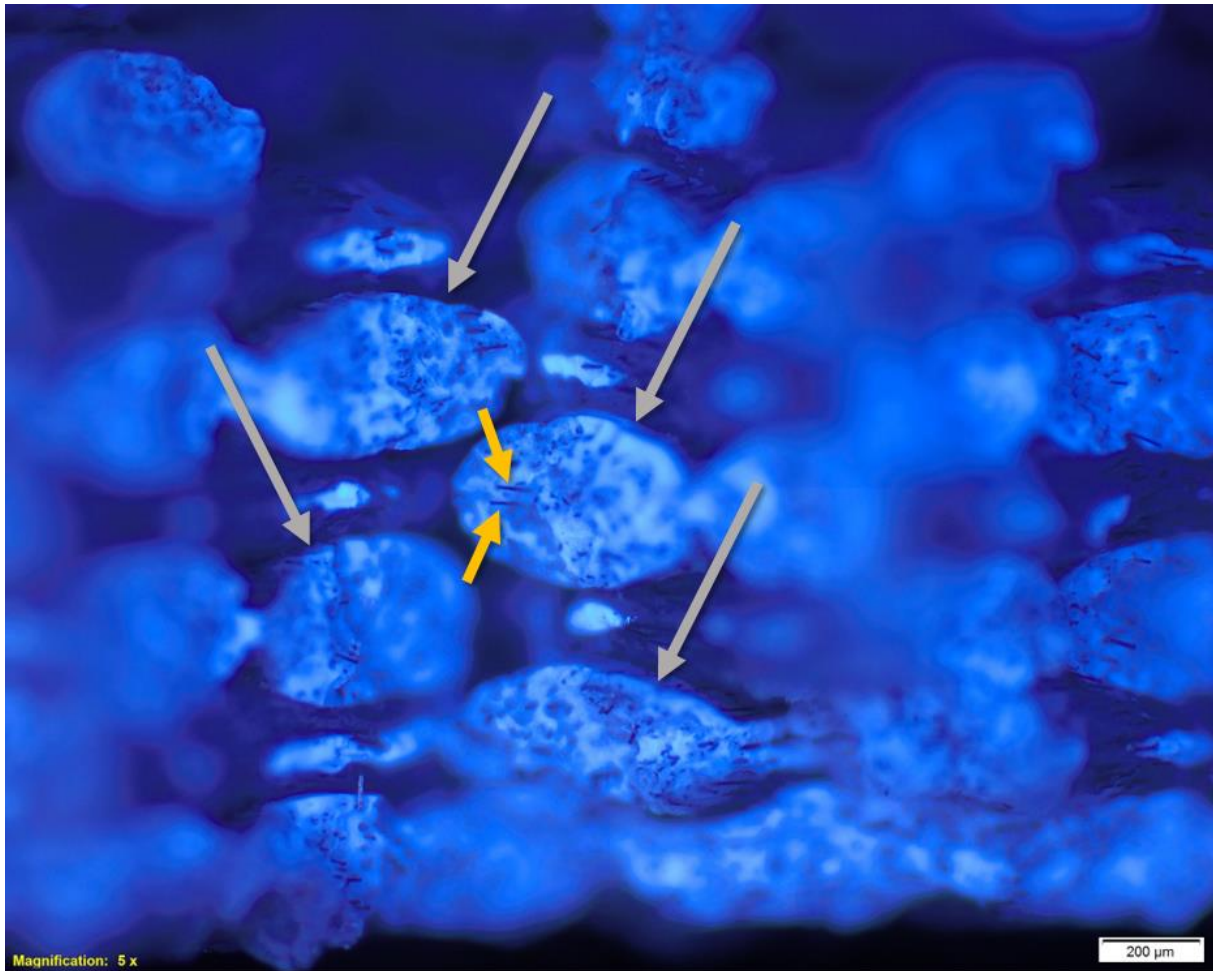


Figure 7 – Fracture of the CF10 sample damaged under tension.

3.4 DMA

Based on the thermogram shown in Fig. 8, it can be observed that as the tested object reaches its glass transition temperature, the storage modulus E' undergoes a significant drop, while the loss modulus E'' peaks. The temperatures corresponding to these transitions are depicted on the graph, along with the values of the respective moduli at temperatures relevant to the extreme operating conditions of passenger aircraft structures. Both samples were fabricated using ABS-CF10 material with 80% infill density. The blue line represents Sparse infill style, while the black line represents Sparse Double Dense infill style. The similar patterns in the graphs for both samples result from the identical material properties. The slightly higher glass transition temperature observed for Sparse Double Dense may be attributed to the greater mass of the sample.

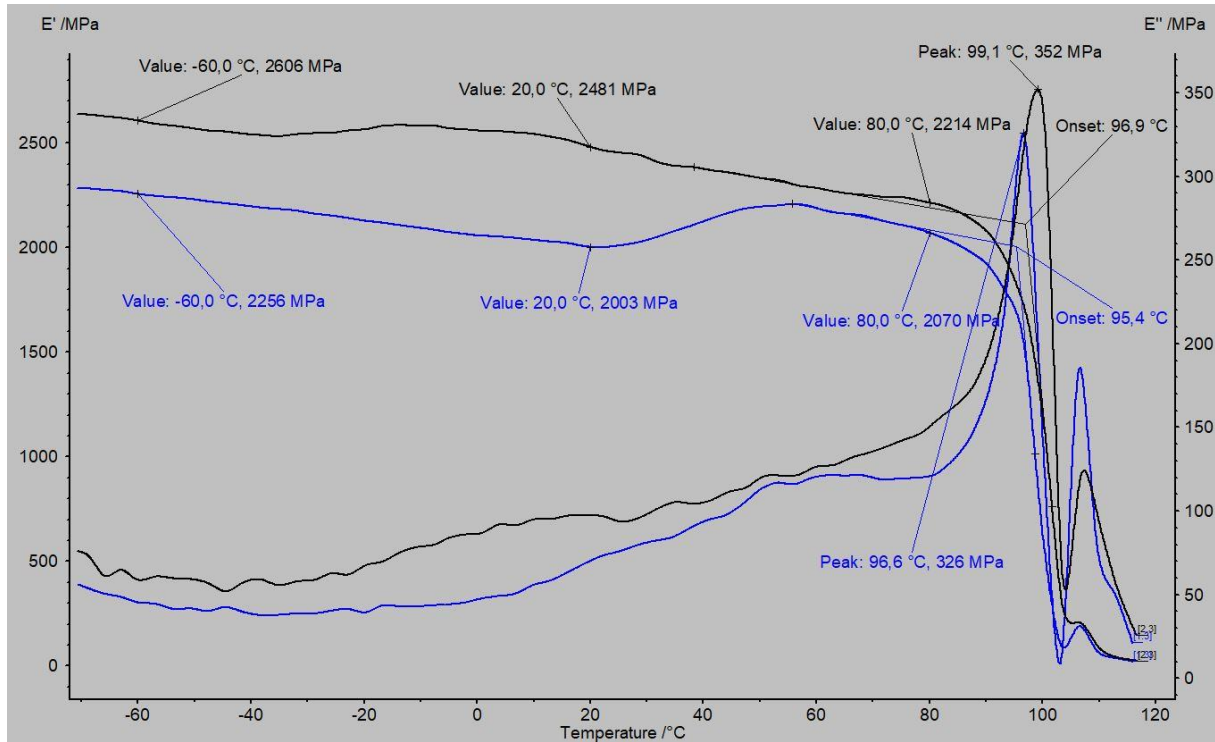


Figure 8 – DMA results for CF10 samples with 80% infill density and different infill styles.

4. Conclusions

Modification of ABS with carbon fiber leads to a notable enhancement in strength and stiffness, albeit with an increase in material density. Optical microscopy allowed for observing the CF10 failure mechanism, which explains the superiority of CF-modified ABS over pure ABS.

Similarly, higher infill density enhances mechanical properties but also raises the structural component's density, a critical consideration in aviation. Depending on the criteria applied, opting for lower infill density may be advantages.

Regarding the effect of infill style on mechanical strength, it can be noted that Sparse Double Dense yields better results while Sparse performs worse for pure ABS. Conversely, for ABS-CF10, Sparse performs better than Sparse Double Dense. DMA studies did not reveal a significant impact of infill style on the thermomechanical properties of CF modified ABS.

5. Copyright Statement

The authors confirm that they, and/or their company or organization, hold copyright on all of the original material included in this paper. The authors also confirm that they have obtained permission, from the copyright holder of any third party material included in this paper, to publish it as part of their paper. The authors confirm that they give permission, or have obtained permission from the copyright holder of this paper, for the publication and distribution of this paper as part of the ICAS proceedings or as individual off-prints from the proceedings.

References

- [1] Kantaros A and Piromalis D. Employing a Low-Cost Desktop 3D Printer: Challenges, and How to Overcome Them by Tuning Key Process Parameters. *International Journal of Mechanics and Applications*, No. 10, pp 11-19, 2021. <https://doi.org/10.5923/j.mechanics.20211001.02>.
- [2] Kantaros A, Papageorgiou M, Brachos K, Ganetsos T & Mouzakiotou S and Soulis E. The Use of 3D Scanning and 3D Color Printing Technologies for the Study and Documentation of Late Bronze Age Pottery from East-Central Greece. *Journal of Mechatronics and Robotics*, No. 8, 2024. <https://doi.org/10.3844/jmrsp.2024.11.19>.
- [3] Fisher T, Almeida Jr H, Falzon BG and Kazancı Z. Tension and Compression Properties of 3D-Printed

EFFECT OF INFILL STYLE AND DENSITY ON MECHANICAL PROPERTIES OF THE CFR ABS MFD FILAMENT

- Composites: Print Orientation and Strain Rate Effects. *Polymers*, No. 15, 1708, 2023.
<https://doi.org/10.3390/polym15071708>.
- [4] Farbman D and McCoy Ch. Materials Testing of 3D Printed ABS and PLA Samples to Guide Mechanical Design. V002T01A015, 2016.
<https://doi.org/10.1115/MSEC2016-8668>.
- [5] Monkova K, Monka P, Hricová R, Hausnerova B and Knapčíková L. Tensile Properties of Four Types of ABS Lattice Structures—A Comparative Study. *Polymers*, No. 15, 4090, 2023.
<https://doi.org/10.3390/polym15204090>.
- [6] Dev S and Srivastava R. Experimental investigation and optimization of the additive manufacturing process through AI-based hybrid statistical approaches. *Progress in Additive Manufacturing*, pp 1-20, 2024.
<https://doi.org/10.1007/s40964-024-00606-z>.
- [7] Głowacki M, Mazurkiewicz A, Skórczewska K, Martínez Valle JM and Smyk E. Change in the Low-Cycle performance on the 3D-Printed Materials ABS, ASA, HIPS, and PLA Exposed to Mineral Oil. *Polymers*, No. 16, 1120, 2024.
<https://doi.org/10.3390/polym16081120>
- [8] Stoklasek P, Navratil M, Bednarik M, Hudec I and Petrzelka D. Flexural behaviour of ABS 3D printed parts on professional printer Stratasys Fortus 900mc. *MATEC Web of Conferences*, No. 210, 04048, 2018.
<https://doi.org/10.1051/mateconf/201821004048>.
- [9] Richkov D, Rosenthal Y, Ashkenazi D and Stern A. Structure and Fracture Visualization of Tilted ABS Specimens Processed via Fused Filament Fabrication Additive Manufacturing. *Annals of Dunarea de Jos University of Galati Fascicle XII Welding Equipment and Technology*, No. 32, pp 5-13, 2021.
<https://doi.org/10.35219/awet.2021.01>.
- [10] Ahmad MN and Yahya A. Effects of 3D Printing Parameters on Mechanical Properties of ABS Samples. *Designs*, No. 7, 136, 2023.
<https://doi.org/10.3390/designs7060136>
- [11] Pervaiz S, Qureshi T, Kashwani G and Kannan S. 3D Printing of Fiber-Reinforced Plastic Composites Using Fused Deposition Modeling: A Status Review. *Materials*, No. 14, 4520, 2021.
<https://doi.org/10.3390/ma14164520>.
- [12] Zhou W and Chen J. 3D Printing of Carbon Fiber Reinforced Plastics and their Applications. *Materials Science Forum*, No. 913, pp 558-563, 2018.
<https://doi.org/10.4028/www.scientific.net/MSF.913.558>.
- [13] Liu W, Huang H, Libin Z and Liu Z. Integrating carbon fiber reclamation and additive manufacturing for recycling CFRP waste. *Composites Part B: Engineering*, No. 215, 108808, 2021.
<https://doi.org/10.1016/j.compositesb.2021.108808>.
- [14] Hu Y, Ladani R, Brandt M, Li Y and Mouritz A. Carbon fibre damage during 3D printing of polymer matrix laminates using the FDM process. *Materials & Design*, No. 205, 2021.
<https://doi.org/10.1016/j.matdes.2021.109679>.
- [15] Abas M, Awadh M, Habib T and Noor S. Analyzing Surface Roughness Variations in Material Extrusion Additive Manufacturing of Nylon Carbon Fiber Composites. *Polymers*, No. 15, 3633, 2023.
<https://doi.org/10.3390/polym15173633>
- [16] Canegrati A, Martulli L, Kostovic M, Rollo G, Sorrentino A, Carboni M and Bernasconi A. Static Behavior of a 3D-Printed Short Carbon Fiber Polyamide: Influence of the Meso-Structure and Water Content. *Materials*, No. 17, 1983, 2024.
<https://doi.org/10.3390/ma17091983>.
- [17] Yan Y, Pillay S and Ning H. Innovative continuous polypropylene fiber composite filament for material extrusion. *Progress in Additive Manufacturing*, pp 1-13, 2024.
<https://doi.org/10.1007/s40964-024-00605-0>.
- [18] Kámán A, Balogh L, Tarcsay B, Jakab M, Meszlényi A, Turcsán T and Egedy A. Glass Fibre-Reinforced Extrusion 3D-Printed Composites: Experimental and Numerical Study of Mechanical Properties. *Polymers*, No. 16, 212, 2024.
<https://doi.org/10.3390/polym16020212>.
- [19] Menard KP, Menard N. *Dynamic Mechanical Analysis*. CRC Press, 2020.